Use of $^{87}Sr/^{86}Sr$ analyses to understand compartmentalisation and the variation of R_w in the Forties reservoir of the Pierce Field, central North Sea

Ross McCartney, Oilfield Water Services Limited, Jackie Kechichian, Gwilym Lynn, Gill Ross, Shell UK Limited.

Abstract

The Pierce Field is a twin diapir structure that produces out of the turbiditic Palaeocene Forties Sandstone Member. Variations in Free Water Level (FWL) and formation water salinity across the field are not completely understood, challenge reservoir management and add uncertainty to reserves estimates. To increase understanding of these variations, $^{87}Sr/^{86}Sr$ ratios of formation water and residual salt analysis (RSA) samples from the oil-leg and underlying aquifer have been interpreted.

The RSA results show that in most wells, $^{87}Sr/^{86}Sr$ ratios increase linearly across the Forties Sandstone from base to top in both the oil-leg and aquifer. The $^{87}Sr/^{86}Sr$ ratios are believed to reflect the composition and flux of fluids entering or diffusing from the underlying Chalk Group and, possibly, overlying Tertiary mudstones into a 'static' Forties reservoir. These conditions appear to have been present during and since oil emplacement.

A good correlation between R_w and $^{87}Sr/^{86}Sr$ ratios in formation water samples has been identified and has been used to estimate R_w at all locations where RSA $^{87}Sr/^{86}Sr$ ratio data are available. This allowed significant improvements to be made to R_w characterisation of the oil-leg across the field which (a) helped minimize the uncertainty in the location of the FWL across the field, (b) has resulted in a change in the calculated S_w distribution in the transition zone and (c) has confirmed the average saturation in the reservoir.

$^{87}Sr/^{86}Sr$ ratios at the base of the Forties have also been classified as Group 1 (Forties-type formation water $^{87}Sr/^{86}Sr$ ratios) or Group 2 (higher $^{87}Sr/^{86}Sr$ ratios). The distribution of these 'Groups' partially correlates with FWL variations and inferred compartment boundaries (sealing faults) and may allow distinction between those boundaries penetrating just the Forties Sandstone and those penetrating both the Chalk Group and the Forties Sandstone Member. This new information may be explored further and incorporated into the next reservoir model for the field.

Integration of formation water salinity and $^{87}Sr/^{86}Sr$ ratio data may improve understanding of variations in formation water salinity in other fields, particularly those with nearby salt.

Introduction

Sr has four stable, naturally-occurring isotopes: ^{84}Sr, ^{86}Sr, ^{87}Sr, and ^{88}Sr. Only ^{87}Sr is radiogenic (i.e. produced by radioactive decay of another isotope) being generated by beta-decay of ^{87}Rb (half-life of 4.88 $\times 10^{10}$ years). $^{87}Sr/^{86}Sr$ ratios have proved useful in a variety of geological investigations. ^{87}Sr and ^{86}Sr are present in oilfield formation water primarily as a result of dissolution of minerals containing ^{87}Sr (e.g. K-feldspar, biotite) and ^{86}Sr (e.g. calcite, plagioclase). $^{87}Sr/^{86}Sr$ ratios can also be changed when formation waters are mixed with the resulting ratios reflecting the Sr content and $^{87}Sr/^{86}Sr$ ratios of the original formation waters.

In oilfield environments, $^{87}Sr/^{86}Sr$ ratio analyses are typically obtained from core samples (residual salt analyses or centrifuged core samples), pre-production formation water samples (e.g. obtained during formation sampling, DST, etc.) or produced water samples (Mearns and McBride, 1999; Smalley et al., 1995). The $^{87}Sr/^{86}Sr$ ratios of the water samples are measured via thermal ionization mass spectrometer (TIMS). These data and their interpretation have a wide range of oilfield applications including:

- Evaluation of hydraulic connectivity and identification of potential barriers to flow in the reservoir (e.g. Mearns and McBride, 1999).
- Characterisation of formation water R_w in the hydrocarbon-leg (e.g. Smalley et al., 1995).
- Identification of hydrodynamic aquifers (e.g. Mearns and McBride, 1999).
- Constraint of basin models (e.g. Barnaby et al., 2004).
- Detection of injection water breakthrough and the quantification of the injection water fraction in produced water (Webb and Kuhn, 2004).
- Identifying the source of produced formation water (e.g. Munz et al., 2010).
- Produced water allocation (e.g. Johansen et al., 2004).

The first two applications above are particularly relevant to the Pierce Field, central North Sea where variations in FWL and formation water salinity are not well understood. In this paper we discuss $^{87}Sr/^{86}Sr$ analyses obtained from core (residual salt analyses), pre-production formation water samples and produced water samples from the Pierce Field and show how their interpretation has increased our understanding of compartmentalisation and the variation of formation water salinity across the field.

Background: Pierce Field

The Pierce Field is located at the eastern margin of the UK Central North Sea (East Central Graben, Blocks 23/22a and 23/27) (Figure 1). It is a twin diapir structure that produces from the turbiditic Palaeocene Forties Sandstone Member (Figure 2). South Pierce was discovered by Ranger Oil in 1975 and North Pierce was discovered by BP in 1990. Oil production began in February 1999 under Enterprise Oil before the asset was acquired by Shell in 2002. The field is currently operated by Shell UK Limited with Summit Petroleum as a partner.

The Forties Sandstone Member was emplaced by turbidity flows influenced by preexisting seafloor topography that funnelled the flows into discrete sediment corridors in the Pierce area (Scott et al., 2010). The 'top' and 'bottom' of the reservoir lie between the maximum flooding surfaces (T80MFS and T70MFS respectively). A top seal is provided by thick Tertiary mudstones of the Stronsay, Westray and Nordland Groups. The reservoir is underlain by non-reservoir shale layers of the Lista and Maureen Formations which, in turn, overlie the Ekofisk, Tor and Hod Formations of the Chalk Group (limestone, marl and chalk). These formations thin up-dip towards the diapirs. The reservoir structure is defined by a series of radial faults radiating outwards from each diapir which introduce some offset of reservoir sands and reduce fluid flow across them. Reservoir quality is approximately 60% net-to-gross, porosity is ~18% and permeability ~15mD. The reservoir is slightly overpressured (250 psi) and contains light oil (38 API) with primary gas caps. The reservoir temperature varies between 99-130^{o}C and the pressure between 300 and 340 bar. The CO_2 content of the oil varies between 0.98 and 1.49 mol%. Seawater injection started in December 2004 and water breakthrough has occurred in several wells.

Variations in FWL have been identified across the reservoir with explanations proposed as either hydrodynamic tilting (Dennis et al., 1998) or by fault compartmentalisation. Whichever mechanism is inferred, FWL depth around the diapirs remains a key uncertainty with respect to reservoir management.

Based on aquifer formation water analyses obtained via drill stem tests (DST) from appraisal wells (23/27-1, 23/27-4, 23/27-6) and from production wells (A1, B1, B2), the aquifer salinity is very variable across the field (between ~53 and possibly up to 386 g/L TDS). The salinity of the lower salinity formation waters are consistent with those occurring in other North Sea Forties reservoirs (45-99 g/L TDS) (unpublished data and Warren and Smalley, 1994) but the higher salinity waters reflect interaction between the formation water and the salt diapirs. The salinity variation across the field is poorly understood and this leads to uncertainties in S_w in the oil-leg and estimated reserves.

^{87}Sr/^{86}Sr data and Cl analyses

Source of data

The majority of the ^{87}Sr/^{86}Sr ratio data for the field has been derived from residual salt analyses undertaken on core samples. Residual salt analysis (RSA) involves crushing a sample of core, and leaching it with de-ionised water for a few minutes. This results in dissolution of any formation water in the pores of the core and any salts that have evaporated from formation water as the cores dry out. The leachate is filtered, passed through a cation exchange column to extract Sr, and the latter is then analysed via thermal ionization mass spectrometry (TIMS) to determine its ^{87}Sr/^{86}Sr ratio. Other studies have demonstrated that unless significant mud invasion has affected the core, the measured ^{87}Sr/^{86}Sr ratio will be representative of the formation water originally present in the core (Mearns and McBride, 1999). Mass spectrometer performance is monitored by analysing NBS (National Bureau of Standards) 987 and Holocene marine carbonate (HMC) standards with the samples.

A total of 177 RSA ^{87}Sr/^{86}Sr ratios have been obtained from Forties core from a total of 9 wells of which 5 are in the water-leg and 4 in the oil-leg (see Figure 3 and Table

1). Other RSA $^{87}Sr/^{86}Sr$ ratios have been obtained from these wells and one additional well (23/27-A10z) from other formations: the Lista (4 ratios), Ekofisk (17), Tor (2) and Hod (1) Formations and from the Forties Sandstone just below the T70MFS in T65 (3) (Table 2).

Good technical conditions existed for obtaining representative formation water $^{87}Sr/^{86}Sr$ ratios from these core samples: reservoir permeabilities are moderate to low, oil-based mud (OBM) was used on most wells and the formation waters contain elevated concentrations of Sr. Only wells 23/27-1 and 23/27-4 were drilled using water-based mud (WBM; KCl polymer). Whilst samples from these wells are thus more likely to show the effects of contamination, the samples were screened using the K/Na ratios of the residual salts and only the least contaminated samples were analysed for their $^{87}Sr/^{86}Sr$ ratio. With the exception of one analysis, the data show good internal consistency (see below) so, with the exception of this one ratio, all the analyses are believed to be of good quality and representative of the formation waters.

$^{87}Sr/^{86}Sr$ ratio and Cl analyses of formation water samples obtained from the aquifer have also been used in this study (Table 3). Produced formation water samples have been obtained from the Forties aquifer of 3 wells (wells A1, B1, B2) (see Figure 3). Wells A1 and B2 produce a mixture of lower and higher salinity formation water and the samples collected probably represent mixtures of the two but with differing fractions of the two waters. A sample of high salinity formation water, contaminated with injected seawater, was also collected from well A1 and modelling has shown that despite the contamination, the $^{87}Sr/^{86}Sr$ ratio of the sample will be representative of the formation water. But, there is significant uncertainty over the Cl content of the formation water (between 124 and 235 mg/L). An additional formation water sample was also obtained from a production test undertaken in the Chalk (23/27-A10z; 168 g/L Cl, $^{87}Sr/^{86}Sr$ ratio = 0.71377).

Pre-production formation water samples were also obtained via DSTs undertaken on the Forties aquifer in three wells (Figure 3). These samples have been analysed for Cl (and other cations and anions). The wells were drilled with KCl WBM (23/27-1, 23/27-4) or $CaCl_2$ OBM (23/27-6). Samples from the former two wells are believed to be of good quality with only minor mud contamination whilst the Cl content of the latter has been estimated after correcting for mud contamination. The samples were not analysed for $^{87}Sr/^{86}Sr$ ratio but it was possible to estimate this ratio in each case from the average RSA $^{87}Sr/^{86}Sr$ ratios obtained from these wells across the depths of the tested zones (see Table 3).

Results

Variation across the Forties Reservoir

Figure 4 shows the Forties RSA $^{87}Sr/^{86}Sr$ ratios against sample depth along with the range of $^{87}Sr/^{86}Sr$ ratios observed in the same reservoir of the Forties Field (0.7084-0.7086) (Warren and Smalley, 1994). It can be seen that some samples from both the oil- and water-legs have compositions similar to the Forties Field formation water but there are many samples that are have ^{87}Sr-enriched $^{87}Sr/^{86}Sr$ ratios. Generally, both oil- and water-leg analyses increase linearly with depth with the exception being the data for well 23/22a-3 which shows a variable trend with depth. One analysis is unusual in that it does not lie on the trend displayed by the other data for that well (sample at 8652.4 ft TVDSS, well 23/22a-2z). This is suspected of being erroneous data and is not considered further.

The linear trends for the different wells appear to have a depth 'offset' so that they do not overlay each other. The lack of overlay could be an artefact of the well trajectories (the wells are deviated) or due to post-emplacement tilting of the reservoir against the diapir (Mearns and McBride, 1999). To remove these effects, the perpendicular distance between the top and the base reservoir and the sample locations was calculated (Figure 5). It was necessary to calculate the distances from both surfaces due to the variable thickness of the Forties Sandstone across the reservoir. Figures 6 and 7 show the Forties RSA $^{87}Sr/^{86}Sr$ ratios plotted against these distances.

It can be seen in Figure 6 that $^{87}Sr/^{86}Sr$ ratios for all wells except 23/22a-3 and 23/27-8 display linear trends across the Forties Sandstone toward the top of the reservoir and several wells are linear to within 45ft or less of top of the reservoir. These trends are displayed by data obtained both in the oil-leg and in the water-leg. Again, the data for well 23/22a-3 display a variable trend with distance below T80MFS whilst the ratios for well 23/27-8 display two linear trends but with different slopes in each case. Despite their different character, the $^{87}Sr/^{86}Sr$ ratios for wells 23/22a-3 and 23/27-8 also display linear trends closer to top reservoir. Based on these results, it is feasible that the $^{87}Sr/^{86}Sr$ ratios of all these wells continue to vary linearly to the top of the reservoir in both the oil-leg and the water-leg. Extrapolating the trends to top reservoir indicates that the $^{87}Sr/^{86}Sr$ ratios at the top of the reservoir are close to ratios observed in the Forties Field for all wells except 23/27-4 (which is higher) (see Table 4).

In Figure 7, again $^{87}Sr/^{86}Sr$ ratios for all the wells display linear trends toward the base of the reservoir and for several wells these data are linear to within 10ft of base reservoir. Extrapolating the trends to base reservoir indicates that the $^{87}Sr/^{86}Sr$ ratios at the base of the reservoir can be separated into two groups (see Table 4). Group 1 includes those wells where the estimated $^{87}Sr/^{86}Sr$ ratio at the base reservoir is close to or slightly higher (0.7086-0.7094) than ratios observed in the Forties Field and Group 2 includes those wells where the estimated ratio is significantly higher (0.7108-0.7119). Each group contains oil-leg and water-leg 'wells'. Other than for well 23/22a-3, the $^{87}Sr/^{86}Sr$ ratios increase linearly from the bottom to the top of the reservoir.

Correlation with salinity

$^{87}Sr/^{86}Sr$ ratios of water-leg formation water samples are positively correlated with 1/Cl so that R_w (estimated from Cl assuming NaCl equivalent; see Table 3) and $^{87}Sr/^{86}Sr$ ratios of the samples are negatively correlated (see Figure 8). Applying linear regression to these results provides the following relationship for the water-leg of the field:

$$R_w = -41.8461.\frac{^{87}Sr}{^{86}Sr} + 29.82294 \qquad \text{Eq. 1}$$

Because the oil- and water-leg RSA $^{87}Sr/^{86}Sr$ ratios have many characteristics in common, it is believed that this equation applies to the oil-leg too. Therefore, along with the increases in $^{87}Sr/^{86}Sr$ ratios from the bottom to the top of the reservoir, formation water salinity will be reducing and R_w increasing. Figure 9 shows the calculated variation in R_w (and associated Cl) above base reservoir for wells 23/27-9 and -10 (Group 1 and 2 wells, respectively). It can be seen that R_w increases linearly from the base of the Forties Formation whilst Cl decreases approximately linearly in well 23/27-9 and curvi-linearly in well 23/27-10.

Discussion: Origin of $^{87}Sr/^{86}Sr$ ratio profiles

RSA $^{87}Sr/^{86}Sr$ ratios for water-leg locations are representative of current formation water compositions and variations within or between wells reflect differences present at this time in the aquifer. Due to the compartmentalised nature of the reservoir and the linearity of the $^{87}Sr/^{86}Sr$ ratios across the Forties Sandstone, it is likely that there is little or no advective flow currently affecting the water-leg in the field. If hydrodynamic conditions did exist, perturbations in the $^{87}Sr/^{86}Sr$ ratio profiles from their linear form might be expected. Linear trends in the ratios are more consistent with diffusive mixing.

The increases in $^{87}Sr/^{86}Sr$ ratios towards base reservoir suggests that there has been, or continues to be, either minor leakage of fluids with higher (than Forties-type formation water) $^{87}Sr/^{86}Sr$ ratios across base reservoir into the Forties reservoir and/or diffusion of strontium isotopes enriched in ^{87}Sr across this zone into the reservoir. Similarly, Cl may be entering the reservoir through base reservoir in the same manner with more Cl entering at the same locations as the ^{87}Sr-enriched components.

There is some evidence to suggest that the fluids entering the Forties through base reservoir and/or the supply of diffusive components have been derived from the underlying formations including the Chalk Group because (see Table 3):

a) Well 23/27-4. $^{87}Sr/^{86}Sr$ ratios continue increasing below base reservoir into the lowermost Forties Formation.

b) Well 23/27-9. Low $^{87}Sr/^{86}Sr$ ratios are present in the underlying Chalk Group and in the overlying Forties Reservoir.

c) Well 23/22a-2. Low $^{87}Sr/^{86}Sr$ ratios are present in the underlying Lista Formation and Chalk Group in an area where low $^{87}Sr/^{86}Sr$ ratios would be expected in the overlying Forties (see below).

It is interesting to note that $^{87}Sr/^{86}Sr$ ratios in the Chalk are higher than expected for formation water in contact with Cretaceous marine carbonates (0.7072-0.7080). This suggests that at least a component of this formation water is likely to have entered the Chalk Group from underlying clastic formations containing K-bearing minerals (e.g. K-feldspar, biotite). In the case of the high $^{87}Sr/^{86}Sr$ ratios present in well 23/27a-A10, this component appears to be large. It may be the flux of fluid entering the Chalk Group from below (and then leaving above) and/or the residence time of these fluids in the Group that can explain the occurrence of Group 1 or 2 $^{87}Sr/^{86}Sr$

ratios at the Forties base reservoir. For example, where Group 1 ratios are observed, the flux of fluid entering the Chalk Group from below might be low and/or the residence time in the Chalk Group may be high so that interaction with marine carbonates lowers, or maintains lower, $^{87}Sr/^{86}Sr$ ratios in the formation water. Similarly, the presence of Group 2 ratios may reflect a high fluid flux into the Chalk Group from below and/or a low residence time of fluids in the Chalk Group so that interaction with marine carbonates does not lower the formation water $^{87}Sr/^{86}Sr$ ratio as much.

Similar processes could be occurring across top reservoir but with ^{87}Sr- and Cl-depleted fluids being involved. But, another possibility is that there is no transfer of Sr isotopes or Cl across this surface and the diffusive mixing observed in the Forties is between (a) existing formation water within the Forties reservoir with a composition similar to that in the Forties Field and (b) those components entering across base reservoir. Under this model, the ^{87}Sr-depleted nature of the formation water at the top reservoir may simply be due to the slow diffusion of ^{87}Sr-enriched components across the reservoir. In support of this suggestion is the ^{87}Sr-enriched formation water of well 23/27-4 at the top of the reservoir. At this location the Forties reservoir is thinner than at any of the other well locations (see Figures 6 and 7) so if diffusion has been occurring for a similar length of time at all locations, it would be anticipated that more of the ^{87}Sr-enriched component would have reached the top reservoir at this location.

Another anomaly in the water-leg data is the ‘break’ in the $^{87}Sr/^{86}Sr$ ratio profile observed in well 23/27-8. However, this coincides with a shaly package on the logs. Therefore, it is likely that this forms a barrier to flow and/or diffusive mixing resulting in the observed offset.

RSA $^{87}Sr/^{86}Sr$ ratios for oil-leg locations are representative of formation water compositions at the time of reservoir filling and variations within or between wells reflect differences present at the time those different locations were filled with oil. For example, an increase in $^{87}Sr/^{86}Sr$ ratios with depth in the oil-leg could reflect an increase in formation water $^{87}Sr/^{86}Sr$ ratios over time as the reservoir fills (Mearns and McBride, 1999). But, in this case, the similarity of the water-leg and oil-leg profiles is striking and it is considered more likely that the ‘static’ conditions hypothesised for the current water-leg were also present when the oil was emplaced. That is, oil was emplaced into a compartmentalised reservoir slowly enough so as not to disturb the $^{87}Sr/^{86}Sr$ ratio profiles but quickly enough for them not to change significantly (via diffusion) during the filling period (i.e. the profiles were ‘frozen’ at the time of emplacement).

The $^{87}Sr/^{86}Sr$ ratios observed in the oil-leg of well 23/22a-3 do not display the simple linear trends of the other wells suggesting that at the time of oil emplacement the conditions suggested for the static model were disturbed. For example, at this location it may be that some fluid flow did occur during oil emplacement, or perhaps oil emplacement was relatively slow in this location so that time-related changes in $^{87}Sr/^{86}Sr$ diffusive mixing of conditions have been captured in the profile.

Given that the Forties Field $^{87}Sr/^{86}Sr$ ratios are similar to the Group 1 ratios, it suggests that on a regional scale, it may be the occurrence of Group 2 ratios at the base of the reservoir that are unusual. If so, it may be that at these locations the local conditions at Pierce are different (e.g. more and deeper seated faulting/fracturing near the diapirs allowing greater flow of fluids from depth into the Chalk?).

Applications

Compartmentalisation

Locations where Group 1 ratios have been observed are often situated within limited geographical areas where other Group 1 ratios have also been observed, and likewise for locations with Group 2 ratios. Also, in some areas there is a change in FWL between wells, and this coincides with a change in the 'Group' between the wells. This raised the possibility that variations in $^{87}Sr/^{86}Sr$ ratio at base reservoir might be related to compartmentalisation in the field and this has been investigated.

Figure 10 shows the distribution of Group 1 and 2 ratios at the base reservoir. Where changes in ratios occur between wells, the possible location where the change occurs has been fixed either where a change in FWL has been identified or where a major fault is present. To complete the distribution map, some additional interpretation of the data was required:

1. Given the low $^{87}Sr/^{86}Sr$ ratios observed in Lista and Chalk samples from well 23/22a-2, it was concluded that this well is likely to have a Group 1 ratio at base reservoir.

2. A formation water sample from well 23/22a-5x contained 62 g/l Cl. Using Equation 1, it was predicted that this formation water would have $^{87}Sr/^{86}Sr$ ratio of ~0.7105 and a Group 2 ratio at base reservoir.

3. Well B2 produces both lower and higher salinity formation water and is cut by a fault which is interpreted to offset the FWL. Although pure samples of these formation waters have not been obtained, to be consistent with the distribution of the $^{87}Sr/^{86}Sr$ ratios it is feasible that the low salinity formation water has a Group 1 ratio and is produced from the toe of the well (nearby wells 23/27-1 and 23/27-5 are in a Group 1 area) meaning the high salinity formation water has a Group 2 ratio and is probably produced from the heel (nearby wells B1, 23/27-6 and 23/27-8 are in a Group 2 area).

4. Well A1 is also cut by a fault which offsets the FWL and it too produces both low and high salinity formation water. Again, to be consistent with the distribution of the $^{87}Sr/^{86}Sr$ ratios it is feasible that the high salinity formation water is produced from the toe of the well (nearby well 23/27-4 is in a Group 2 area) suggesting the lower salinity formation water is being produced from the heel (nearby well 23/27-9 is in a Group 1 area).

In Figure 10 it can be seen that three types of fault are present with respect to the change in FWL and Group type:

- Type A. Here there is a change in FWL across the fault and a change in

Group.

- Type B. No change in FWL across the fault but a change in Group.
- Type C. A change in FWL across the fault and no change in Group.

One possible explanation for these observations is that they may be related to the vertical extent or variable transmissibility with depth of faults. This is schematically portrayed in Figure 11. It can be seen that where the fault penetrates through the Forties and Chalk (Type A fault), a change in FWL and Group is expected across the fault. Where the fault only penetrates through the Chalk (Type B fault) or is only open to flow in the Forties, a change in FWL is not expected but a change in Group should be observed (although there may be mixing between the low and high ratio water in the Forties above the sealing fault). Finally, where the fault only penetrates through the Forties (Type C fault) or is only open to flow in the Chalk, a change in FWL is expected but not a change in Group.

The information on possible subsurface conditions gained through interpretation of the variation in $^{87}Sr/^{86}Sr$ ratios at the base reservoir within the context of a compartmentalised reservoir has provided possible insights into variable transmissibility with depth of faults in the field and indicates that the Group 2 areas may be better connected to underlying formations and hence provide migration routes into the Forties reservoir. This information will be explored further and may be included when and if a new reservoir model is constructed.

Oil-leg formation water resistivity

Previously, the R_w model for the oil-leg at Pierce allowed for some variation of salinity based on the variation observed in water-leg formation water samples but the model was fairly rudimentary.

The RSA $^{87}Sr/^{86}Sr$ ratios have now been used to generate R_w profiles using Equation 1 for each of the wells for which there are oil-leg data. These profiles have then been extrapolated to estimate R_w across the reservoir in the oil-leg. The revised R_w model has improved understanding of oil saturation and pressures in the field. For example:

1. New water gradients have been developed for RFT pressures and this has helped minimize the uncertainty in the location of the Free Water Level (FWL) across the field.

2. Log saturations have been recalculated using the variable R_w data. Although this has not changed the average saturation across the field it has changed S_w distribution in the transition zone.

3. A new saturation height function has been calculated independently from core and compared with the newly calculated log saturations. There is a good match between the results which supports the validity of using Equation 1 in the oil-leg of the field.

Implications for other fields

The salinities of formation waters have been found to be variable in other fields producing from the Forties Formation. For example, the Forties Field (25-60 g/L Cl) (Coleman, 2011) and the Nelson Field (54-62 g/L Cl) (Gill et al., 2010). But, the salinity variation at Pierce is much greater which is likely to be related to the proximity of salt. This significant salinity variation has been beneficial in that it has resulted in a strong R_w-$^{87}Sr/^{86}Sr$ ratio correlation for the formation waters. It may be, therefore, that the integration of R_w and $^{87}Sr/^{86}Sr$ ratio data may be a particularly useful tool for fields located near salt. Particularly because under these conditions it is likely that variable R_w will be present in the reservoirs and so may affect calculated saturations.

In this study we made use of formation water analyses to determine the relationship between R_w and $^{87}Sr/^{86}Sr$ ratios in the water-leg, and then applied this to the oil-leg. In other fields the relationship in the oil-leg may be different from that in the water-leg, or water-leg data may not be available. In these cases, the relationship between R_w and $^{87}Sr/^{86}Sr$ ratios in the oil-leg could, perhaps, be obtained directly from Dean-Stark Crush and Leach core samples (Clinch et al., 2010; Pan, 2005) which have been analysed for both Cl and $^{87}Sr/^{86}Sr$ ratios.

Conclusions

- $^{87}Sr/^{86}Sr$ analyses obtained from core (residual salt analyses), pre-production formation water samples and produced water samples from the Pierce Field have been evaluated and interpreted.

- These have shown that generally formation water $^{87}Sr/^{86}Sr$ ratios decrease linearly from the base to the top of the Forties reservoir in both the oil-leg and water-leg.

- A correlation between $^{87}Sr/^{86}Sr$ ratios and salinity (and resistivity) has been identified in the water-leg of the reservoir such that formation water salinity must also decrease (and R_w increase) from the base to the top of the Forties reservoir in both the oil-leg and water-leg.

- The $^{87}Sr/^{86}Sr$ ratio profiles across the reservoir are believed to be the result of minor leakage of fluids, or diffusion of components (Na, Cl, Sr isotopes) into a 'static' reservoir, from formations underlying the reservoir and, possibly, those overlying. These conditions appear to have been present during and since oil emplacement.

- Some areas of the field appear to have higher salinity, ^{87}Sr-rich fluids or components entering the Forties reservoir across its base and these may be indicative of areas that are better connected to underlying formations and hence provide migration routes into the Forties reservoir.

- The results of the study have allowed an improved R_w model for the oil-leg to be developed which has helped minimize the uncertainty in the location of the

Free Water Level (FWL) across the field, has changed S_w distribution in the transition zone, and confirmed the average oil saturation for the field.

- The results have also generated new information regarding the potential extent of sealing faults in the reservoir which may be explored and incorporated into the next reservoir model for the field.

- Integration of formation water salinity and $^{87}Sr/^{86}Sr$ ratio data may improve understanding of variations in formation water salinity in other fields, particularly those with nearby salt.

Acknowledgements

The authors are grateful to Shell UK Limited and the partner in the Pierce Field (Summit Petroleum) for permission to publish this paper. We also thank Isotopic Limited (John McBride) for undertaking the residual salt extractions and for performing the $^{87}Sr/^{86}Sr$ analyses on these extractions, and on the produced formation water samples.

References

Barnaby, R.J., Oetting, G.C., Gao, G., 2004. Strontium isotopic signatures of oil-field waters: Applications for reservoir characterisation. Amer. Assoc. Petrol. Geol. Bull. 88, 1677-1704.

Clinch, S., Wei, W., Lasswell, P., Shafer, J.L., 2010. Determining formation water salinity in the oil leg using cores and logs, 51st SPWLA Annual Logging Symposium, Perth, Australia, p. 15.

Coleman, M.L., 2011. Dramatic variations in oil zone and aquifer water compositions in Forties and Gyda Fields, Infatuation with saturation. London Petrophysical Society, London.

Gill, C.E., Shepherd, M., Millington, J.J., 2010. Compartmentalisation of the Nelson Field, Central North Sea: evidence from produced water chemistry analysis, in: Jolley, S.J., Fisher, Q.J., Ainsworth, R.B., Vrolijk, P.J., Delisle, S. (Eds.), Reservoir compartmentalisation. Geological Society of London, pp. 71-87.

Johansen, H., Ramstad, K., Rein, E., 2004. Monitoring involving formation water history, 15th International Oil Field Chemistry Symposium. Tekna, Geilo, Norway.

Mearns, E.W., McBride, J.J., 1999. Hydrocarbon filling history and reservoir continuity of oil fields evaluated using $^{87}Sr/^{86}Sr$ isotope ratio variations in formation water, with examples from the North Sea. Petrol. Geosci. 5, 17-27.

Munz, I.A., Johansen, H., Huseby, O., Rein, E., Scheire, O., 2010. Water flooding of the Oseberg Øst oil field, Norwegian North Sea: Application of formation water chemistry and isotopic composition for production monitoring. Marine and Petroleum Geology 27, 838-852.

Pan, C., 2005. Determination of connate water salinity from preserved core, International Symposium of the Society of Core Analysts, Toronto, Canada, p. 13.

Scott, E.D., Gelin, F., Jolley, S.J., Leenaarts, E., Sadler, S.P., Elsinger, R.J., 2010. Sedimentological control of fluid flow in deep marine turbidite reservoirs:

Pierce Field, UK Central North Sea. Geological Society, London, Special Publications 347, 113-132.
Smalley, P.C., Dodd, T.A., Stockden, I.L., Raheim, A., Mearns, E.W., 1995. Compositional heterogeneities in oilfield formation waters: identifying them, using them, in: Cubitt, J.M., England, W.A. (Eds.), The Geochemistry of Reservoirs. The Geological Society, London.
Warren, E.A., Smalley, P.C., 1994. North Sea Formation Water Atlas, Geological Society Memoir No. 15. Geological Society, London, p. 208.
Webb, P.J., Kuhn, O., 2004. Enhanced scale management through the application of inorganic geochemistry and statistics, 6th International Symposium on Oilfield Scale. Society of Petroleum Engineers, Aberdeen, Scotland.

Table 1 RSA $^{87}Sr/^{86}Sr$ ratio analyses for the Forties Sandstone Member (between bottom and top reservoir).

Well	Depth (TVDSS ft)	$^{87}Sr/^{86}Sr$	Perpendicular distance below top reservoir (ft)	Perpendicular distance above bottom reservoir (ft)	Leg
23/27-1	9202.30	0.70865	82.96	509.69	Water-leg
23/27-1	9218.50	0.70864	102.96	489.69	Water-leg
23/27-1	9288.00	0.70859	175.65	417.00	Water-leg
23/27-1	9324.50	0.70860	210.65	382.00	Water-leg
23/27-1	9358.50	0.70860	245.65	347.00	Water-leg
23/27-1	9417.50	0.70875	305.65	287.00	Water-leg
23/27-1	9440.00	0.70873	325.65	267.00	Water-leg
23/27-1	9453.90	0.70874	340.65	252.00	Water-leg
23/27-1	9495.50	0.70879	380.65	212.00	Water-leg
23/27-1	9541.50	0.70883	425.65	167.00	Water-leg
23/27-4	8858.60	0.70982	14.36	170.54	Water-leg
23/27-4	8881.10	0.71011	46.44	138.47	Water-leg
23/27-4	8892.60	0.71032	56.44	128.47	Water-leg
23/27-4	8907.00	0.71040	71.44	113.47	Water-leg
23/27-4	8926.50	0.71064	86.44	98.47	Water-leg
23/27-4	8931.00	0.71075	91.44	93.47	Water-leg
23/27-4	8947.00	0.71101	106.44	78.47	Water-leg
23/27-4	8984.40	0.71169	174.18	10.72	Water-leg
23/27-5	8942.50	0.70837	32.01	318.54	Water-leg
23/27-5	8972.30	0.70843	62.01	288.54	Water-leg
23/27-5	8996.20	0.70840	87.01	263.54	Water-leg
23/27-5	9022.20	0.70840	109.95	240.60	Water-leg
23/27-5	9047.30	0.70840	133.30	217.25	Water-leg
23/27-5	9066.70	0.70841	153.30	197.25	Water-leg
23/27-5	9089.10	0.70846	178.30	172.25	Water-leg
23/27-5	9113.40	0.70853	198.30	152.25	Water-leg
23/27-5	9116.40	0.70851	203.30	147.25	Water-leg
23/27-5	9148.20	0.70852	233.30	117.25	Water-leg
23/27-5	9169.00	0.70852	258.30	92.25	Water-leg
23/27-5	9184.40	0.70852	273.30	77.25	Water-leg
23/27-6	9597.70	0.70947	122.82	266.03	Water-leg
23/27-6	9613.60	0.70960	142.82	246.03	Water-leg

Well	Depth (TVDSS ft)	$^{87}Sr/^{86}Sr$	Perpendicular distance below top reservoir (ft)	Perpendicular distance above bottom reservoir (ft)	Leg
23/27-6	9632.50	0.70971	157.82	231.03	Water-leg
23/27-6	9653.40	0.70987	182.82	206.03	Water-leg
23/27-6	9672.80	0.71003	202.82	186.03	Water-leg
23/27-6	9693.20	0.71020	222.82	166.03	Water-leg
23/27-6	9714.10	0.71036	242.82	146.03	Water-leg
23/27-6	9735.00	0.71056	262.82	126.03	Water-leg
23/27-6	9747.40	0.71066	282.82	106.03	Water-leg
23/27-6	9772.30	0.71080	302.82	86.03	Water-leg
23/27-8	8130.90	0.70902	60.03	257.48	Water-leg
23/27-8	8133.90	0.70908	60.03	257.48	Water-leg
23/27-8	8137.90	0.70904	64.97	252.54	Water-leg
23/27-8	8143.40	0.70911	69.29	248.23	Water-leg
23/27-8	8149.40	0.70918	75.35	242.17	Water-leg
23/27-8	8155.40	0.70924	77.85	239.67	Water-leg
23/27-8	8162.30	0.70925	82.54	234.98	Water-leg
23/27-8	8172.30	0.70937	95.97	221.54	Water-leg
23/27-8	8176.30	0.70940	100.97	216.54	Water-leg
23/27-8	8184.80	0.70953	105.97	211.54	Water-leg
23/27-8	8188.30	0.70957	110.97	206.54	Water-leg
23/27-8	8192.20	0.70957	115.97	201.54	Water-leg
23/27-8	8197.70	0.70966	120.97	196.54	Water-leg
23/27-8	8200.70	0.70970	125.97	191.54	Water-leg
23/27-8	8203.20	0.70972	125.97	191.54	Water-leg
23/27-8	8220.10	0.70981	140.97	176.54	Water-leg
23/27-8	8303.90	0.71035	235.97	81.54	Water-leg
23/27-8	8305.90	0.71034	235.97	81.54	Water-leg
23/27-8	8312.80	0.71036	245.97	71.54	Water-leg
23/27-8	8319.80	0.71042	250.97	66.54	Water-leg
23/27-8	8322.80	0.71041	255.97	61.54	Water-leg
23/27-8	8327.30	0.71044	260.97	56.54	Water-leg
23/27-8	8331.80	0.71048	265.97	51.54	Water-leg
23/27-8	8338.20	0.71059	270.77	46.75	Water-leg
23/27-9	7499.38	0.70846	72.83	99.53	Oil-leg
23/27-9	7507.42	0.70846	86.04	86.32	Oil-leg
23/27-9	7517.46	0.70842	118.43	53.93	Oil-leg
23/27-9	7526.96	0.70850	138.43	33.93	Oil-leg
23/27-9	7537.87	0.70856	158.09	14.27	Oil-leg
23/27-9	7546.33	0.70856	168.09	4.27	Oil-leg
23/27-9	7553.60	0.70858	175.59	3.23	Oil-leg
23/27-9	7562.30	0.70856	183.09	10.73	Oil-leg
23/27-9	7573.20	0.70855	200.07	27.71	Oil-leg
23/27-10	8365.40	0.70911	120.53	385.19	Oil-leg
23/27-10	8375.70	0.70919	130.53	375.19	Oil-leg
23/27-10	8384.50	0.70926	140.53	365.19	Oil-leg
23/27-10	8402.20	0.70934	160.53	345.19	Oil-leg
23/27-10	8415.10	0.70942	175.53	330.19	Oil-leg
23/27-10	8424.40	0.70946	185.53	320.19	Oil-leg
23/27-10	8431.30	0.70953	190.53	315.19	Oil-leg
23/27-10	8438.70	0.70954	200.53	305.19	Oil-leg

Well	Depth (TVDSS ft)	$^{87}Sr/^{86}Sr$	Perpendicular distance below top reservoir (ft)	Perpendicular distance above bottom reservoir (ft)	Leg
23/27-10	8446.50	0.70961	215.53	290.19	Oil-leg
23/27-10	8455.10	0.70966	225.53	280.19	Oil-leg
23/27-10	8463.70	0.70974	230.53	275.19	Oil-leg
23/27-10	8475.10	0.70981	245.53	260.19	Oil-leg
23/27-10	8489.40	0.70993	260.53	245.19	Oil-leg
23/27-10	8532.70	0.71020	312.20	202.44	Oil-leg
23/27-10	8542.00	0.71026	322.20	192.44	Oil-leg
23/27-10	8556.10	0.71035	337.20	177.44	Oil-leg
23/27-10	8557.70	0.71038	342.20	172.44	Oil-leg
23/27-10	8568.40	0.71042	352.20	162.44	Oil-leg
23/27-10	8582.70	0.71050	367.20	147.44	Oil-leg
23/27-10	8585.80	0.71053	372.20	142.44	Oil-leg
23/22A-2Z	8652.40	0.70956	39.95	374.74	Oil-leg
23/22A-2Z	8658.40	0.70842	44.95	369.74	Oil-leg
23/22A-2Z	8663.90	0.70843	49.95	364.74	Oil-leg
23/22A-2Z	8666.90	0.70842	49.95	364.74	Oil-leg
23/22A-2Z	8670.80	0.70842	54.95	359.74	Oil-leg
23/22A-2Z	8674.30	0.70845	59.95	354.74	Oil-leg
23/22A-2Z	8678.30	0.70845	59.95	354.74	Oil-leg
23/22A-2Z	8684.30	0.70846	69.95	344.74	Oil-leg
23/22A-2Z	8690.80	0.70847	74.95	339.74	Oil-leg
23/22A-2Z	8701.70	0.70851	84.95	329.74	Oil-leg
23/22A-2Z	8703.70	0.70849	84.95	329.74	Oil-leg
23/22A-2Z	8721.20	0.70857	99.95	314.74	Oil-leg
23/22A-2Z	8727.20	0.70859	104.95	309.74	Oil-leg
23/22A-2Z	8732.60	0.70857	109.64	305.05	Oil-leg
23/22A-2Z	8740.60	0.70860	117.46	297.23	Oil-leg
23/22A-2Z	8746.10	0.70862	121.19	293.50	Oil-leg
23/22A-2Z	8755.10	0.70864	126.80	287.89	Oil-leg
23/22A-2Z	8758.00	0.70863	129.30	285.39	Oil-leg
23/22A-2Z	8767.00	0.70864	137.42	277.27	Oil-leg
23/22A-2Z	8774.00	0.70869	145.16	269.53	Oil-leg
23/22A-2Z	8780.00	0.70873	150.16	264.53	Oil-leg
23/22A-2Z	8784.90	0.70869	155.16	259.53	Oil-leg
23/22A-2Z	8797.90	0.70875	165.16	249.53	Oil-leg
23/22A-2Z	8807.40	0.70881	175.16	239.53	Oil-leg
23/22A-2Z	8816.80	0.70878	185.16	229.53	Oil-leg
23/22A-2Z	8835.80	0.70888	200.16	214.53	Oil-leg
23/22A-2Z	8839.30	0.70885	205.16	209.53	Oil-leg
23/22A-2Z	8845.80	0.70886	210.16	204.53	Oil-leg
23/22A-2Z	8853.70	0.70890	220.16	194.53	Oil-leg
23/22A-2Z	8868.20	0.70888	230.16	184.53	Oil-leg
23/22A-2Z	8882.10	0.70895	245.16	169.53	Oil-leg
23/22A-2Z	8893.60	0.70896	255.16	159.53	Oil-leg
23/22A-3	8821.50	0.70869	81.97	407.13	Oil-leg
23/22A-3	8838.00	0.70874	96.97	392.13	Oil-leg
23/22A-3	8845.90	0.70876	106.97	382.13	Oil-leg
23/22A-3	8848.90	0.70878	111.97	377.13	Oil-leg
23/22A-3	8850.90	0.70878	111.97	377.13	Oil-leg

Well	Depth (TVDSS ft)	$^{87}Sr/^{86}Sr$	Perpendicular distance below top reservoir (ft)	Perpendicular distance above bottom reservoir (ft)	Leg
23/22A-3	8861.20	0.70876	125.50	363.60	Oil-leg
23/22A-3	8867.30	0.70880	130.26	358.84	Oil-leg
23/22A-3	8874.70	0.70880	135.26	353.84	Oil-leg
23/22A-3	8879.20	0.70882	140.26	348.84	Oil-leg
23/22A-3	8884.20	0.70884	145.26	343.84	Oil-leg
23/22A-3	8888.70	0.70883	150.26	338.84	Oil-leg
23/22A-3	8893.70	0.70892	155.26	333.84	Oil-leg
23/22A-3	8906.10	0.70885	170.26	318.84	Oil-leg
23/22A-3	8915.50	0.70884	175.26	313.84	Oil-leg
23/22A-3	8920.50	0.70887	180.26	308.84	Oil-leg
23/22A-3	8928.00	0.70886	190.26	298.84	Oil-leg
23/22A-3	8933.40	0.70891	195.26	293.84	Oil-leg
23/22A-3	8940.40	0.70888	200.26	288.84	Oil-leg
23/22A-3	8944.40	0.70885	205.26	283.84	Oil-leg
23/22A-3	8956.30	0.70890	220.26	268.84	Oil-leg
23/22A-3	8962.30	0.70889	225.26	263.84	Oil-leg
23/22A-3	8967.30	0.70890	230.26	258.84	Oil-leg
23/22A-3	8977.70	0.70889	245.26	243.84	Oil-leg
23/22A-3	8982.20	0.70890	245.26	243.84	Oil-leg
23/22A-3	8988.20	0.70891	255.26	233.84	Oil-leg
23/22A-3	8995.10	0.70891	260.26	228.84	Oil-leg
23/22A-3	8999.10	0.70888	265.26	223.84	Oil-leg
23/22A-3	9006.10	0.70890	275.26	213.84	Oil-leg
23/22A-3	9013.00	0.70887	280.26	208.84	Oil-leg
23/22A-3	9018.50	0.70888	285.26	203.84	Oil-leg
23/22A-3	9024.50	0.70888	290.26	198.84	Oil-leg
23/22A-3	9030.90	0.70888	300.26	188.84	Oil-leg
23/22A-3	9040.90	0.70886	310.26	178.84	Oil-leg
23/22A-3	9044.90	0.70887	315.26	173.84	Oil-leg
23/22A-3	9048.30	0.70883	320.26	168.84	Oil-leg
23/22A-3	9053.30	0.70885	325.26	163.84	Oil-leg
23/22A-3	9064.30	0.70882	335.26	153.84	Oil-leg
23/22A-3	9071.20	0.70879	340.26	148.84	Oil-leg
23/22A-3	9076.70	0.70880	350.26	138.84	Oil-leg
23/22A-3	9086.10	0.70876	360.26	128.84	Oil-leg
23/22A-3	9090.60	0.70877	365.26	123.84	Oil-leg
23/22A-3	9098.10	0.70874	370.26	118.84	Oil-leg
23/22A-3	9109.50	0.70871	385.26	103.84	Oil-leg
23/22A-3	9117.00	0.70866	390.26	98.84	Oil-leg
23/22A-3	9124.40	0.70862	400.26	88.84	Oil-leg
23/22A-3	9132.40	0.70865	410.26	78.84	Oil-leg
23/22A-3	9149.30	0.70862	425.26	63.84	Oil-leg
23/22A-3	9155.70	0.70863	435.26	53.84	Oil-leg
23/22A-3	9169.40	0.70871	450.26	38.84	Oil-leg
23/22A-3	9178.60	0.70873	455.26	33.84	Oil-leg
23/22A-3	9199.00	0.70880	480.26	8.84	Oil-leg
23/22A-3	9214.90	0.70882	497.22	8.12	Oil-leg

Table 2 RSA $^{87}Sr/^{86}Sr$ ratio analyses for other locations.

Well	Depth (TVDSS ft)	$^{87}Sr/^{86}Sr$	Location
23/27-4	8998.90	0.71205	Forties below bottom reservoir
23/27-4	9020.40	0.71229	Forties below bottom reservoir
23/27-9	7588.52	0.70862	Forties below bottom reservoir
23/27-9	7684.80	0.70862	Ekofisk
23/27-9	7694.13	0.70861	Ekofisk
23/27-9	7705.45	0.70860	Ekofisk
23/27-9	7716.90	0.70862	Ekofisk
23/27-9	7725.25	0.70859	Ekofisk
23/27-9	7733.64	0.70858	Ekofisk
23/27-9	7743.52	0.70856	Ekofisk
23/27-9	7746.29	0.70860	Tor
23/27-9	7748.66	0.70859	Tor
23/22A-2	7669.30	0.70834	Lista
23/22A-2	7673.60	0.70832	Lista
23/22A-2	7676.50	0.70841	Lista
23/22A-2	7681.90	0.70833	Lista
23/22A-2	7888.50	0.70818	Hod
23/27a-A10	8209.25	0.71211	Ekofisk
23/27a-A10	8214.95	0.71218	Ekofisk
23/27a-A10	8222.22	0.71206	Ekofisk
23/27a-A10	8227.50	0.71239	Ekofisk
23/27a-A10	8232.26	0.71219	Ekofisk
23/27a-A10	8237.03	0.71237	Ekofisk
23/27a-A10	8241.73	0.71189	Ekofisk
23/27a-A10	8245.93	0.71232	Ekofisk
23/27a-A10	8250.09	0.71233	Ekofisk
23/27a-A10	8254.06	0.71274	Ekofisk

Table 3 $^{87}Sr/^{86}Sr$ ratio and Cl analyses and estimated R_w for aquifer formation water samples.

Well	$^{87}Sr/^{86}Sr \pm \sigma$	Cl ± σ (mg/L)	R_W (ohm.m), 60°F
23/27-1	0.7087±0.0001	29.7	0.163
23/27-4	0.7108±0.0009	73.1	0.078
23/27-6	0.7092±0.0005	26.55±6.55	0.181
A1 (mixed FW)	0.70860	30.0	0.162
A1 (high salinity FW)	0.71150	179.5±55.5	0.042
B1	0.70989	40.4	0.126
B2 (mixed FW)	0.70884	32.5	0.151
B2 (mixed FW)	0.70919	37.9	0.133

Table 4 Estimated $^{87}Sr/^{86}Sr$ ratios at top and bottom reservoir.

Well	Top reservoir $^{87}Sr/^{86}Sr$	Bottom reservoir $^{87}Sr/^{86}Sr$	Bottom reservoir Group
23/27-1	0.70853	0.70890	Group 1
23/27-4	0.70961	0.71185	Group 2
23/27-5	0.70834	0.70859	Group 1
23/27-6	0.70851	0.71147	Group 2
23/27-8	0.70843	0.71080	Group 2
23/27-8	0.70894	0.71162	Group 2
23/27-10	0.70843	0.71138	Group 2
23/27-9	0.70836	0.70857	Group 1
23/22A-2Z	0.70828	0.70942	Group 1
23/22A-3	0.70858	0.70881	Group 1

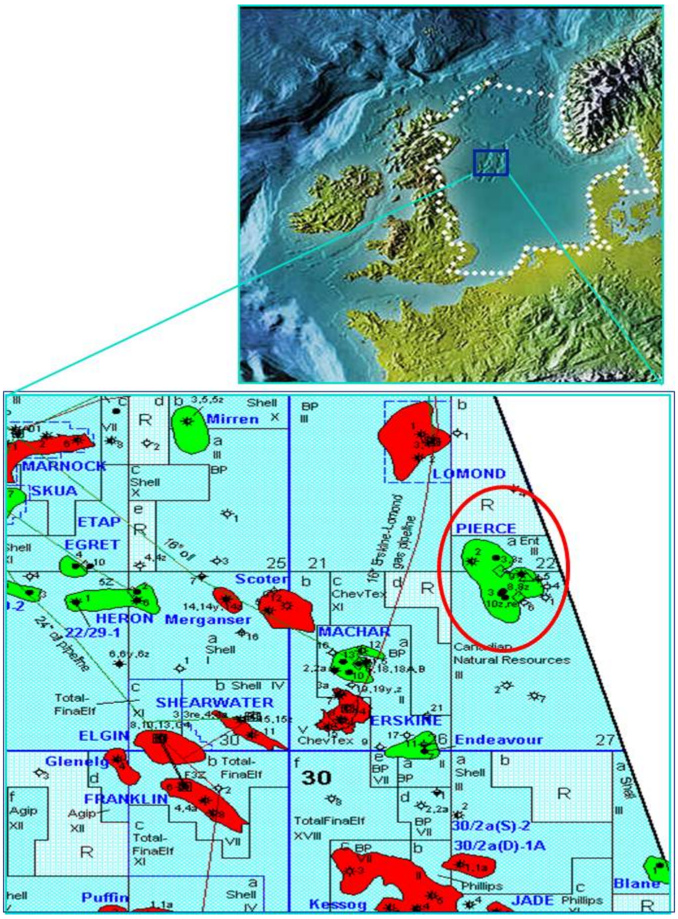

Figure 1 Location of the Pierce Field.

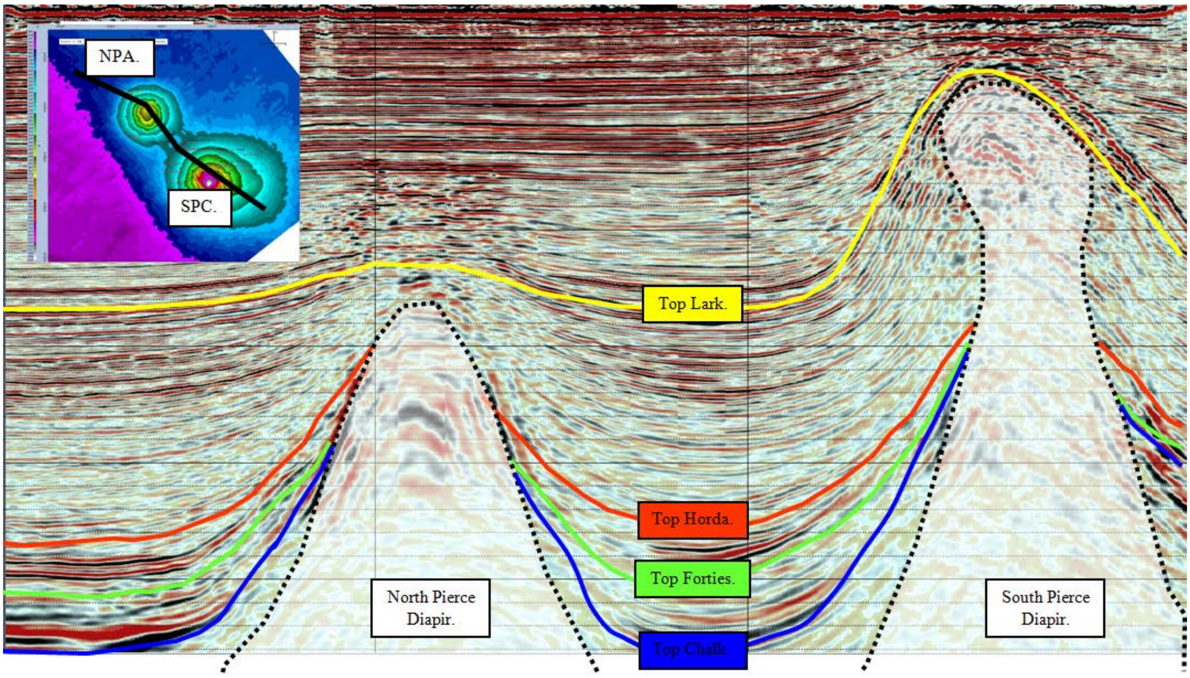

Figure 2 Seismic cross-section of the Pierce Field.

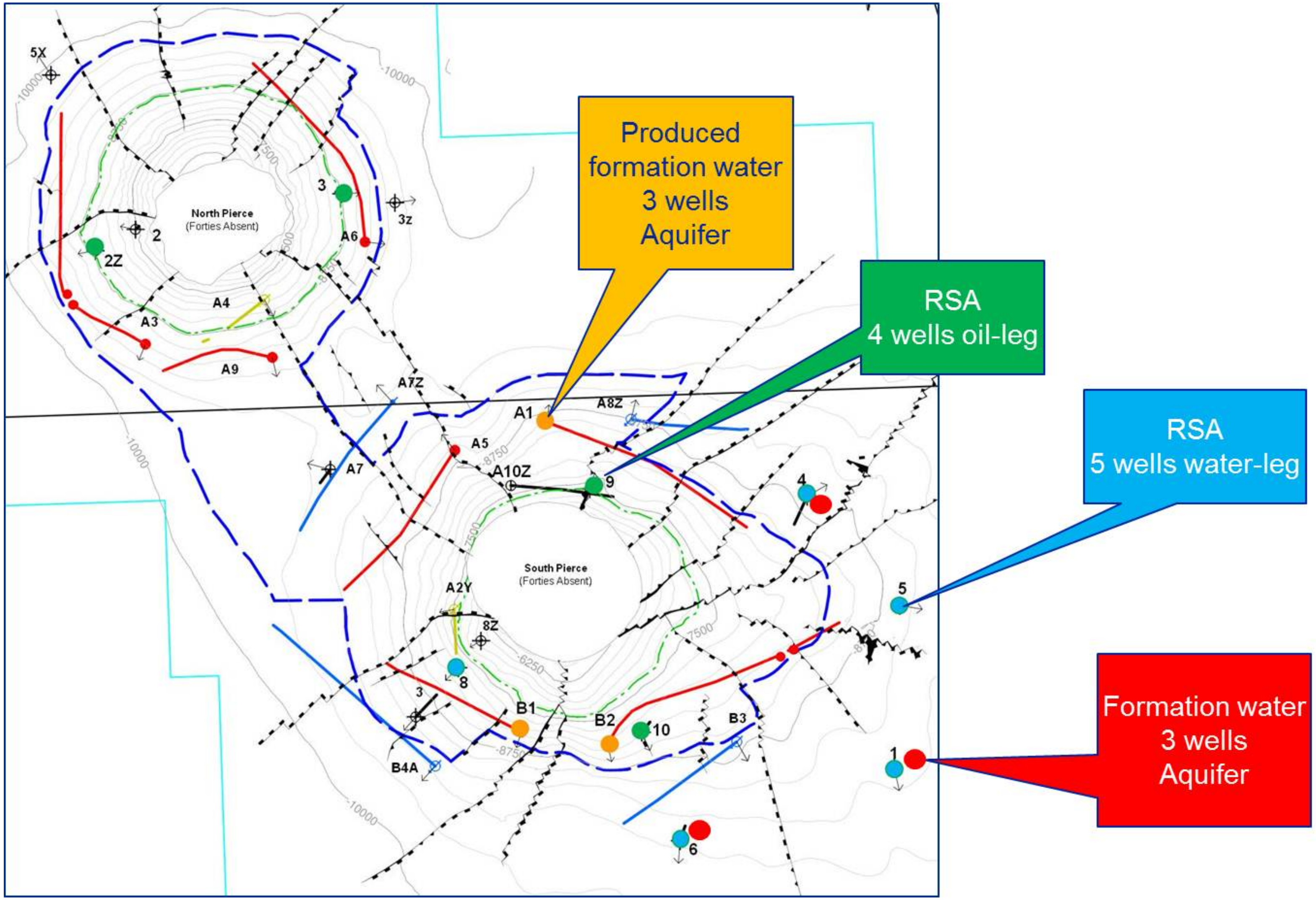

Figure 3 Distribution of $^{87}Sr/^{86}Sr$ ratio data from the Pierce Field. Dashed blue line shows location of FWL. Dashed black lines show location of faults.

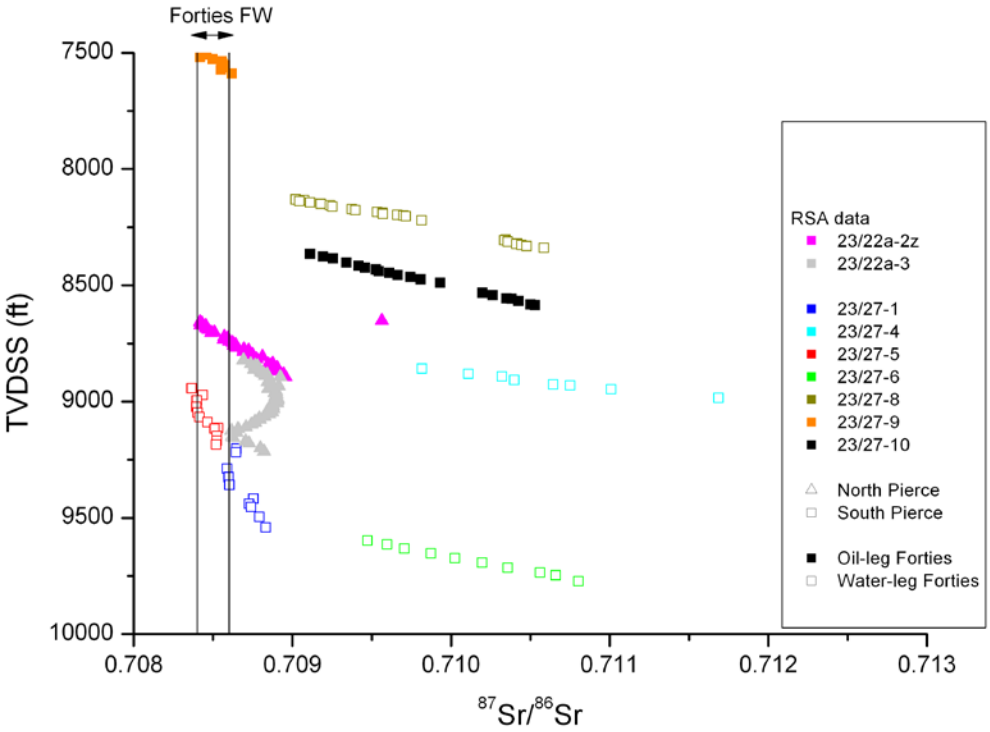

Figure 4 Variation of Forties RSA $^{87}Sr/^{86}Sr$ ratios with depth.

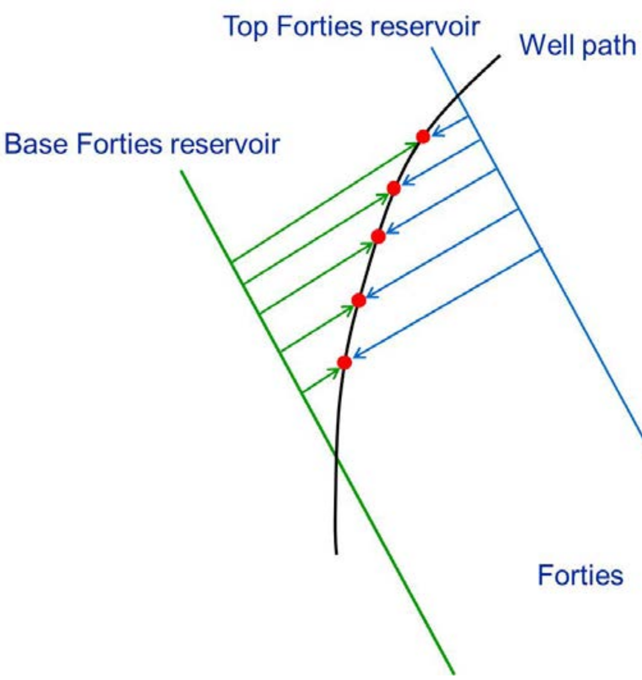

Figure 5 Schematic representation of the calculation of perpendicular distances between top and bottom reservoir and RSA sample locations.

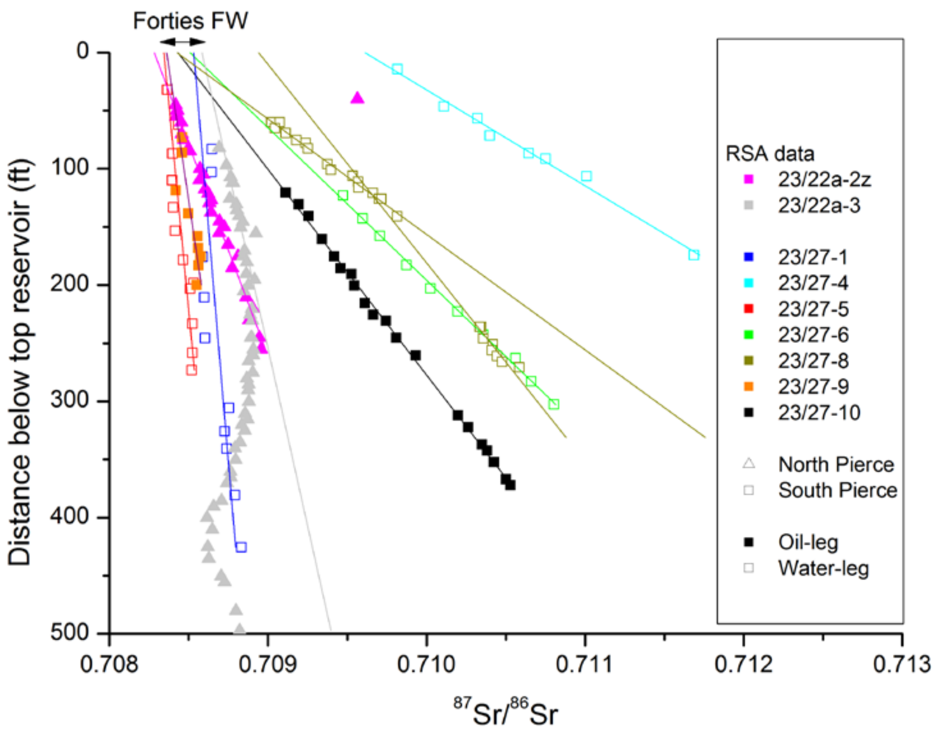

Figure 6 Variation of Forties RSA $^{87}Sr/^{86}Sr$ ratios with perpendicular distance below top reservoir.

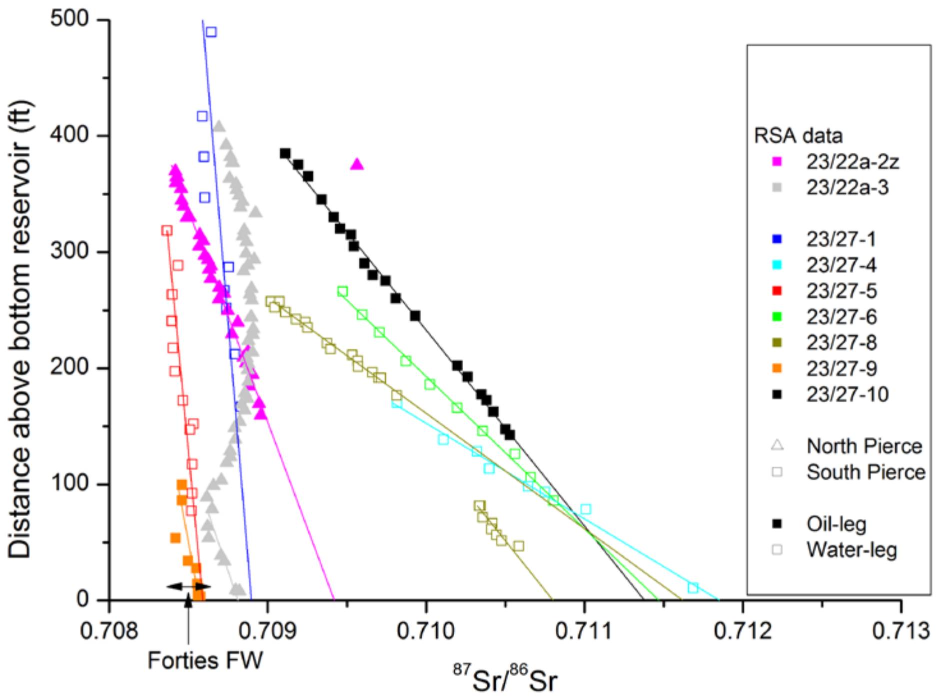

Figure 7 Variation of Forties RSA $^{87}Sr/^{86}Sr$ ratios with perpendicular distance above base reservoir.

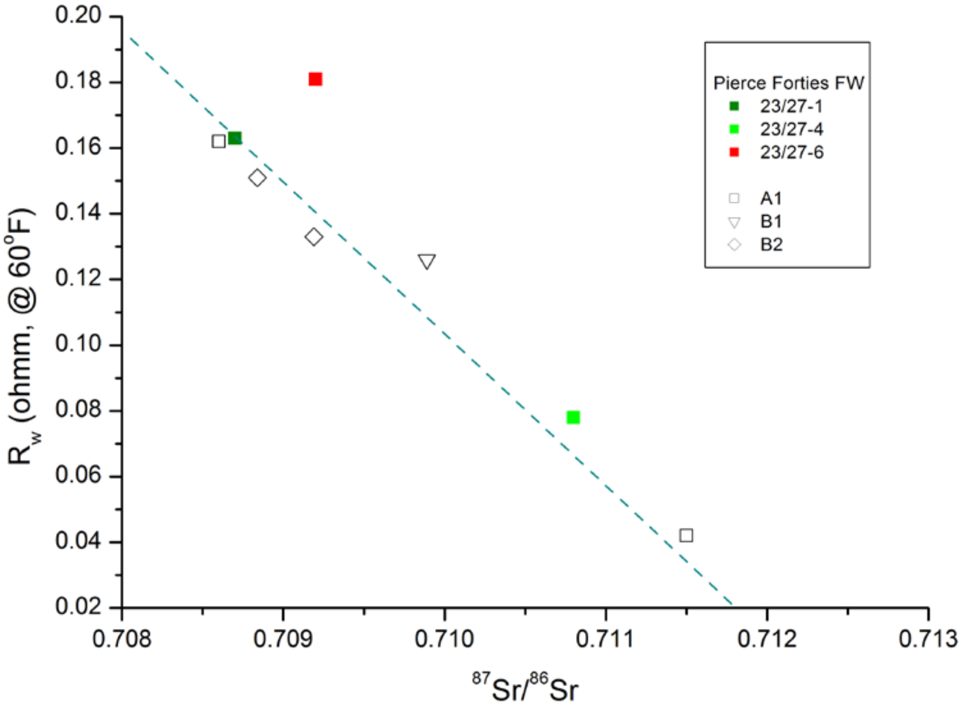

Figure 8 Variation of water-leg formation water $^{87}Sr/^{86}Sr$ with R_w.

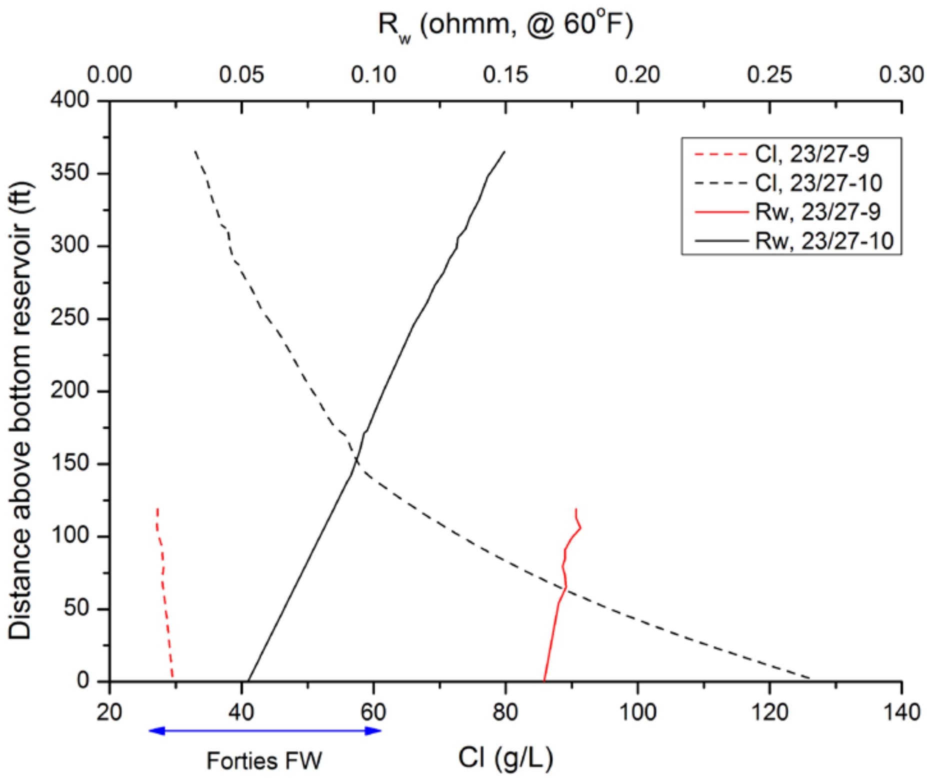

Figure 9 Variation of formation water Cl and R_w perpendicularly across the Forties reservoir from bottom reservoir in wells 23/27-9 and -10.

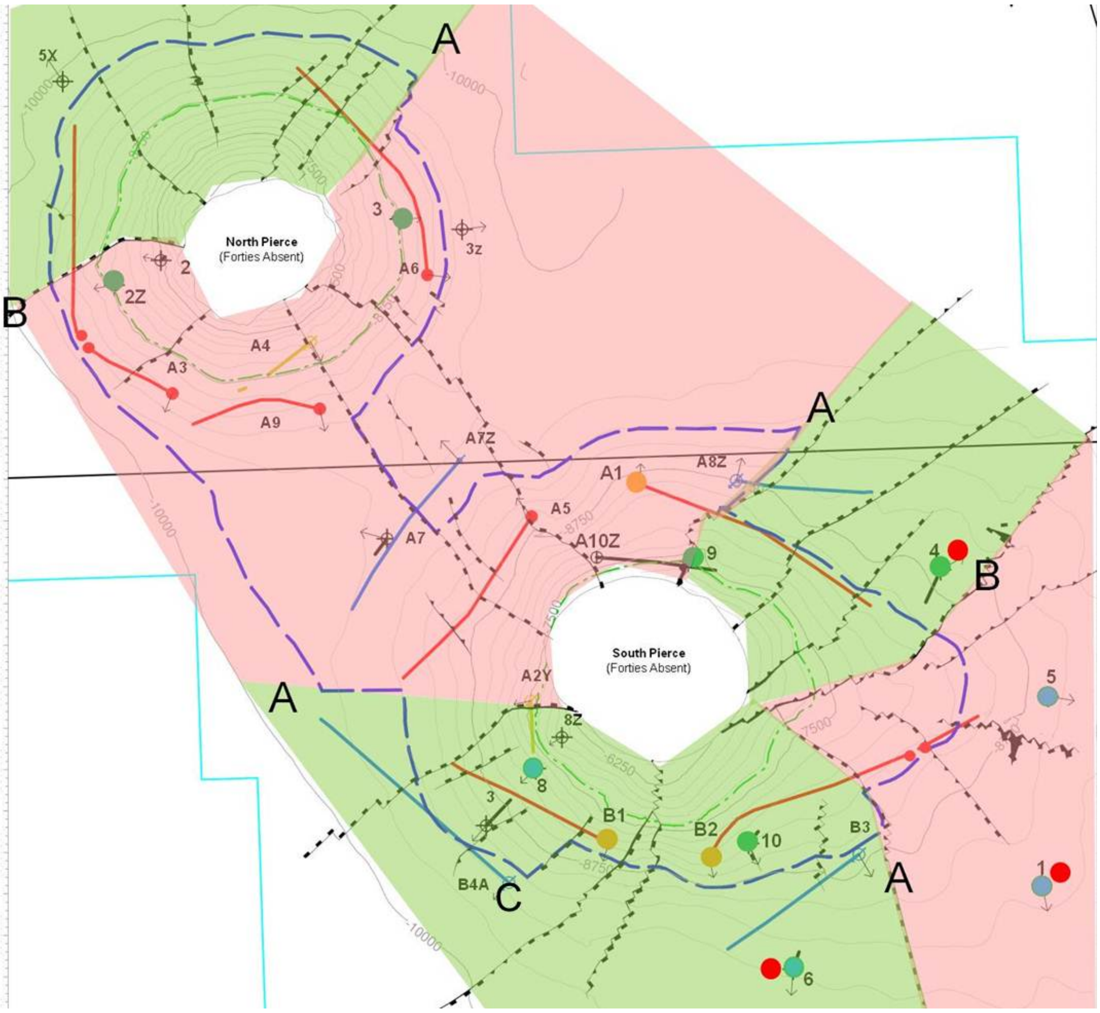

Figure 10 Distribution of areas where Group 1 (green) and Group 2 (pink) wells are located and the relationship of these areas with changes in FWL (A, B, C – see main text for explanation).

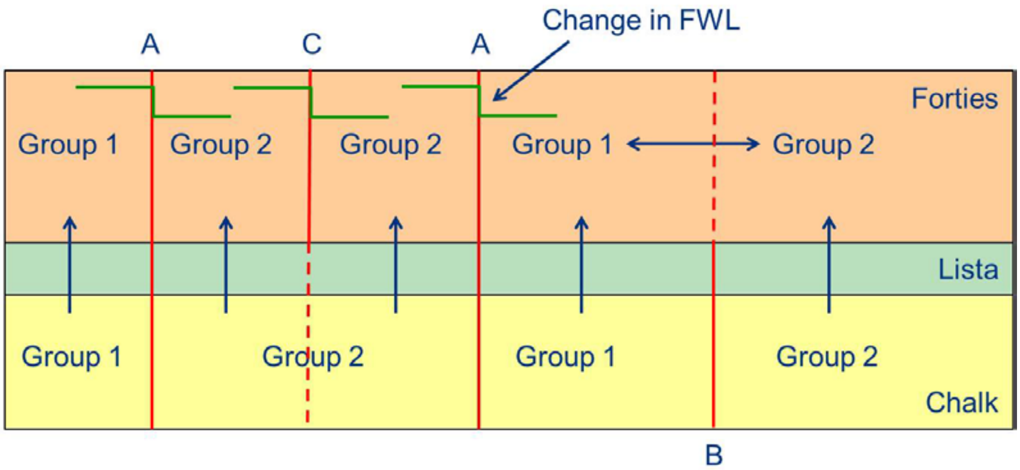

Figure 11 Schematic diagram explaining the potential relationship between faults, changes in FWL and observed $^{87}Sr/^{86}Sr$ ratios at bottom reservoir (see main text for explanation) (A, B, C = types of fault).